

# A Comparative Study of PSO, GWO, and HOA Algorithms for Maximum Power Point Tracking in Partially Shaded Photovoltaic Systems

Research paper

Fares Berttahir\*<sup>ORCID</sup>, Sabrina Abdeddaim, Achour Betka, Charrouf Omar

LGEB, University of Mohamed Khidar, Biskra, Algeria

Received: 24 July, 2023; Accepted: 16 January 2024

**Abstract:** Solar energy harnessed through photovoltaic technology plays a crucial role in generating electrical energy. Maximising the power output of solar modules requires optimal solar radiation. However, challenges arise due to obstacles such as stationary objects, buildings, and sand-laden winds, resulting in multiple points of maximum power on the P-V curve. This problem requires the use of maximum power point tracking algorithms, especially in unstable climatic conditions and partial shading scenarios. In this study, we propose a comparative analysis of three MPPT methods: particle swarm optimisation (PSO), grey wolf optimisation (GWO) and Horse Herd Optimization Algorithm (HOA) under dynamic partial shading conditions. We evaluate the accuracy of these methods using Matlab / Simulink simulations. The results show that all three methods solve partial shading problems effectively and with high precision. Furthermore, the Horse Herd Optimization approach has superior tracking accuracy and faster convergence compared with the other proposed methods.

**Keywords:** grey wolf optimization (GWO) • horse herd optimization algorithm (HOA) • maximum power point tracking (MPPT) • partial shading • particle swarm optimization (PSO) • photovoltaic generation systems

## 1. Introduction

The increasing energy demands across industries and sectors have created a pressing need for electrical energy (Krishna et al., 2015). However, the reliance on fossil fuels like oil and coal is contributing to global warming and environmental degradation (Bollipo et al., 2020). As a result, there is a growing demand for sustainable and renewable energy sources. Photovoltaic (PV) energy, derived from solar power, offers a promising solution. It is a clean and abundant renewable energy resource suitable for residential, industrial, and commercial applications (Yang et al., 2018).

Photovoltaic (PV) cells are at the forefront of renewable energy technology, possessing a unique ability to directly convert light energy from the sun into electrical energy (Bhukya et al., 2018). However, an inherent challenge in solar energy utilization lies in the potential obstruction of sunlight, which can impede the efficient harnessing of the received solar energy. This obstruction can manifest as shadows, clouds, buildings or tree leaves that cast shadows on the PV cell surface. When sunlight is partially blocked, multiple peak power points may occur within the nonlinear current-voltage (I-V) and power-voltage (P-V) characteristics of the PV cell (Hanafiah et al., 2017).

These peak power points include the global maximum power point (GMPP) and local maximum power points (LMPP). Attaining and maintaining the GMPP, especially in the presence of numerous LMPPs, is essential to ensure optimal energy conversion from the PV module. To address this challenge, the implementation of a technology called Maximum Power Point Tracking (MPPT) becomes necessary. The MPPT system continually and dynamically determines the GMPP of the PV module in real time, adapting to varying weather conditions and other environmental factors (Li et al., 2019).

\* Email: fares.bettahar@univ-biskra.dz

The MPPT system optimizes the output power of the PV module by intelligently adjusting its operating point, ensuring that it consistently operates at or near the GMPP. This optimization is crucial for maximizing the energy harvest from the solar panels and enhancing the overall system efficiency (Chauhan et al., 2019). By employing MPPT technology, solar PV systems can effectively counter the fluctuating nature of solar radiation and shadows, enhancing their performance and making them more reliable sources of clean and sustainable energy.

The literature presents a wide array of Maximum Power Point Tracking (MPPT) methods, in (Baba et al., 2020) extensively covering these methodologies. These approaches are categorized based on various criteria such as tracking speed efficiency, cost, and complexity. However, the effectiveness of a specific MPPT technique is contingent upon its ability to accurately track the maximum power point, especially amidst rapidly changing weather conditions. Consequently, techniques are further classified based on their tracking nature specifically in the context of Partially Shaded Photovoltaic Solar Cells. Author is referenced as (Subudhi and Pradhan 2013, Ahmad et al., 2019) offer detailed discussions on all these techniques, which are broadly grouped into three classifications: Classical MPPT, Intelligent MPPT, and Optimization MPPT. This classification provides valuable insights for selecting and implementing the most appropriate MPPT technique, considering the unique requirements and circumstances associated with partially shaded PSCs.

For classical MPPT as reviewed by (Ahmed et al., 2015), the techniques include fractional open-circuit voltage (FOCV), fractional short-circuit current (FSCC), hill climbing (HC).constant voltage (CV) adaptive reference voltage (ARV), ripple correlation control (RCC) lookup, In addition to the previously mentioned classifications, two widely recognized traditional MPPT methods are Perturb and Observe (P&O) (Hota et al., 2017) and Incremental Conductance (INC) (Jately et al., 2021). Both of these methods rely on instantaneous power and conductance values for their operation, adjusting the duty cycle to track the Maximum Power Point (MPP) these techniques are readily implementable due to their algorithmic simplicity (Motahhir et al., 2018). They prove highly efficient under uniform irradiation conditions, wherein the PV system typically produces a singular Global Maximum Power Point (GMPP). However, research by (Chellal et al., 2021) suggests that P&O and INC methods struggle to effectively track the MPP under varying irradiation conditions. They often have difficulty differentiating between the Global Maximum Power Point (GMPP) and Local Maximum Power Points (LMPP).

Shading can significantly influence the performance of photovoltaic (PV) systems, leading to energy losses and reducing overall efficiency. It was found that 41% of installed PV systems were affected by shading, resulting in approximately 10% energy loss (Wang et al., 2016). In response to the urgent need to address shading-related energy losses, extensive research efforts have been invested in the further development and fine-tuning of Maximum Power Point Tracking (MPPT) technologies in recent years. Researchers are actively working on improving MPPT algorithms with the aim of improving their robustness and adaptability to a range of environmental conditions, particularly partial shading scenarios.

Various Soft Computing (SC) techniques include artificial intelligence (AI) (Yung et al., 2020 and Yadav et al., 2022) have been developed, such as fuzzy logic control (FLC), artificial neural networks (ANN), adaptive neuro-fuzzy inference system (ANFIS), Machine learning and Deep Reinforcement Learning based MPPT. These sophisticated methods are specifically tailored to adapt to dynamic weather conditions, ensuring highly accurate Maximum Power Point Tracking (MPPT). They exhibit exceptional tracking efficiencies and speeds. However, it is important to note that these methods often involve complex control circuitry and extensive data processing for training the system in advance.

The Fuzzy Logic Controller (FLC) is a widely used non-linear control technique for implementing Maximum Power Point Tracking (MPPT) in solar photovoltaic systems. FLC does not require prior knowledge of the system's dynamics for efficient MPPT. Within FLC, two prevalent design methods are the Mamdani (M) and Taguchi-Sukeno (T-S) methods. The Mamdani-based FLC has been successfully implemented for MPPT, as documented in (Naick et al., 2017). This FLC-based MPPT controller has demonstrated superior performance, particularly in rapidly tracking the optimal Maximum Power Point (MPP) even under varying solar irradiation conditions. On the other hand, in (Villegas-Mier et al., 2021), the authors discuss advantages and limitations of using ANNs in MPPT, analysing various ANN-based MPPT techniques and comparing their performance with traditional algorithms for optimal power tracking. Although offering faster tracking, requires a significant amount of training data to achieve enhanced accuracy. This technique utilizes dynamic irradiation and temperature as inputs, storing them as datasets. As is the case in Machine learning (Memaya et al., 2019 and Khan et al., 2023). Deep Reinforcement Learning based MPPT (Phan et al., 2020).

In recent years, the use of metaheuristic optimization approaches has increased significantly (Nassef et al., 2023). These metaheuristic methods provide a way to mitigate the drawbacks of both conventional and AI-based MPPT techniques. Recent research has introduced several metaheuristic optimization methods that are widely used in solving complex optimization challenges in engineering and various other critical fields. Some of the most used metaheuristic optimization methods in literature are Particle Swarm Optimization (PSO), Firefly Algorithm (FA), Artificial Bee Colony (ABC), Cuckoo Search (CS), Flower Pollination Algorithm (FPA), Grey Wolf Optimization (GWO), Mine Blast Optimization (MBO), Salp Swarm Algorithm (SSA), Dragonfly Optimization Algorithm (DFO), Harmony Search Algorithm (HSA), Genetic Algorithm (GA), Sine–Cosine Algorithm (SCA) and Bat Algorithm (BA). Among others. These algorithms have greater stability and adapt efficiently to varying environmental conditions and system parameters. Their robustness when dealing with complex and nonlinear optimization landscapes further adds to their attractiveness. In addition, metaheuristic algorithms are characterized by global optimization and ensure the identification of the true MPP in the operating range of the system. Their adaptability and ability to find an efficient balance between exploration and exploitation make them versatile tools for optimizing MPPT in renewable energy systems.

The main objective of this work is to study and conduct a comprehensive comparative analysis of three different algorithms for tracking the Global Maximum Power Point (GMPP) of a photovoltaic (PV) system under the influence of partial shading. The algorithms considered are Particle Swarm Optimization (PSO), Grey Wolf Optimization (GWO) and Horse Herd Optimization Algorithm (HOA). The research aims to provide a holistic understanding of their performance under dynamic partial shading conditions. Through a rigorous evaluation and comparison of these algorithms, we aim to make a significant contribution to the broader field of Maximum Power Point Tracking (MPPT) technologies in the context of photovoltaic systems. The aim is to offer a balanced assessment of their respective strengths and weaknesses. We use Matlab/Simulink for validation and the full analysis of the results is detailed in the full research report.

## 2. Model of the PV generator

A PV cell can be described as a current source that generates an  $I_{ph}$  current proportional to the amount of light and heat that occurs. According to the single-diode model, Figure 1 depicts the equivalent circuit of a solar cell (Peng et al., 2018). The current at the output of the cell is given by the equation when Kirchhoff's law is applied. The mathematical equations are described as (Kumar and Rao, 2016):

$$I_{pv} = I_{ph} - I_d \quad (1)$$

The following equation relates the generated photocurrent  $I_{ph}$  to the solar irradiation.

$$I_{ph} = \frac{G}{G_r} (I_{sc} + K_i (T - T_r)) \quad (2)$$

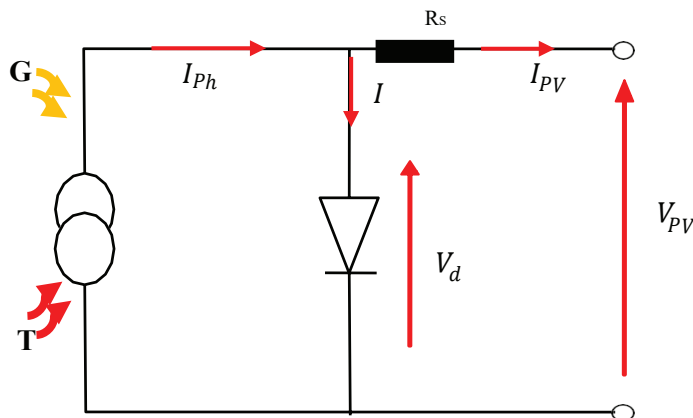


Fig. 1. Equivalent circuit of solar PV module.

The diode current is given as:

$$V_d = V_{pv} + R_s I_{pv} \quad (3)$$

$$I_d = I_o \left( \exp \left( \frac{V_d}{V_{th}} \right) - 1 \right) \quad (4)$$

On the other hand, the cell saturation current and thermal voltage, which is described as, follows:

$$I_o = I_{sc} - I_{op} \left[ \exp \left( \frac{-(V_{op} + R_s I_{op})}{V_{th}} \right) \right] \quad (5)$$

$$V_{th} = \frac{(V_{op} + R_s I_{op} - V_{oc})}{\log \left( 1 - \frac{I_{op}}{I_{sc}} \right)} \quad (6)$$

Where:

$I_{ph}$ : the current generated by light.

$I_{pv}$ : Cell output current (A).

$I_d$ : the current of the diode.

$V_{op}$ : Voltage of Pmax (V).

$V_{pv}$ : Cell output voltage (V).

$V_{th}$ : the thermal voltage of the module.

$I_{op}$ : Current of Pmax (A).

$V_{oc}$ : Open circuit voltage.

$I_o$ : the reverse saturation current in amperes (A).

$R_s$ : Series resistance.

$I_{sc}$ : the short-circuit current.

$K_i$ : the temperature coefficient of the cell short-circuit current (=0.0013A/C).

$T_r$ : the reference temperature of the cell, in Kelvin (K) (=25 °C + 273).

$G$ : the solar radiation in watt/square meter (W/m<sup>2</sup>).

$G_r$ : the reference insolation of the cell (=1000 W/m<sup>2</sup>).

The electrical characteristics under standard conditions ( $G= 1000\text{W/m}^2$ , and  $T=25^\circ\text{C}$ ) of the photovoltaic module used for the simulations are presented in Table 1.

**Table 1.** Specification of the solar panel

Parameters	Variable	Value
Short circuit current	$I_{sc}$	5.4A
Open circuit voltage	$V_{oc}$	44 V
Current of $P_{max}$	$I_{op}$	4.95 A
Voltage of $P_{max}$	$V_{op}$	35.4 V
Maximum power	$P_{op}$	175 W
Series resistance	$R_s$	0.5 $\Omega$

### 3. Characteristics Of PV Modules under Partial Shading

Multiple solar modules arranged in both series and parallel combinations are what make up a PV array. The series connection is meant to raise the output voltage. On the contrary, parallel connections dramatically raise the overall current output, which is an essential factor in effectively powering electrical equipment (Li et al., 2023). The production phase of solar energy presents a potential challenge in the form of hot spots. These local temperature

increases can significantly affect the performance and longevity of the system. To eliminate this problem, a bypass diode is strategically integrated into the module connections. This diode serves as a crucial preventive measure to effectively mitigate hot spot problems and maintain system reliability and durability. However, the exploitation of large spaces by solar panels for electricity production makes them susceptible to partial shading caused by factors such as clouds, buildings, trees or sandstorms. Such shading can lead to problems in the PV system, as modules may receive varying levels of irradiance, resulting in energy loss. In addition, they create multiple points in a curve (P-V).

In order to understand this behaviour of solar panels, two random PV array configurations are illustrated in Figures 2 and 3. Figure 2 shows a 4S configuration illustrating the connection of four modules in a series

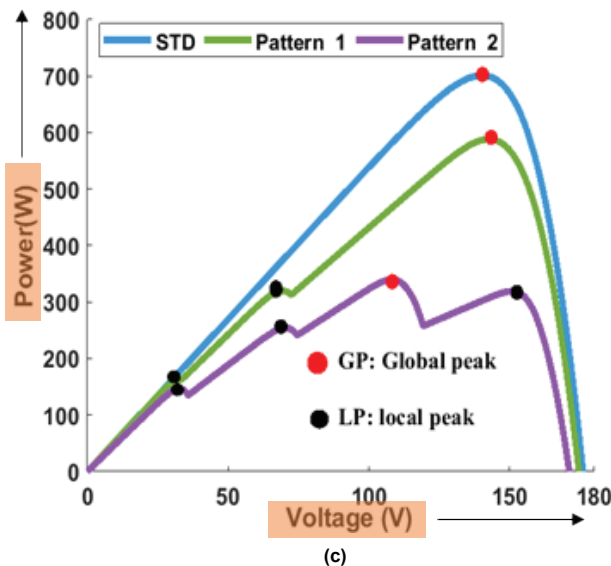
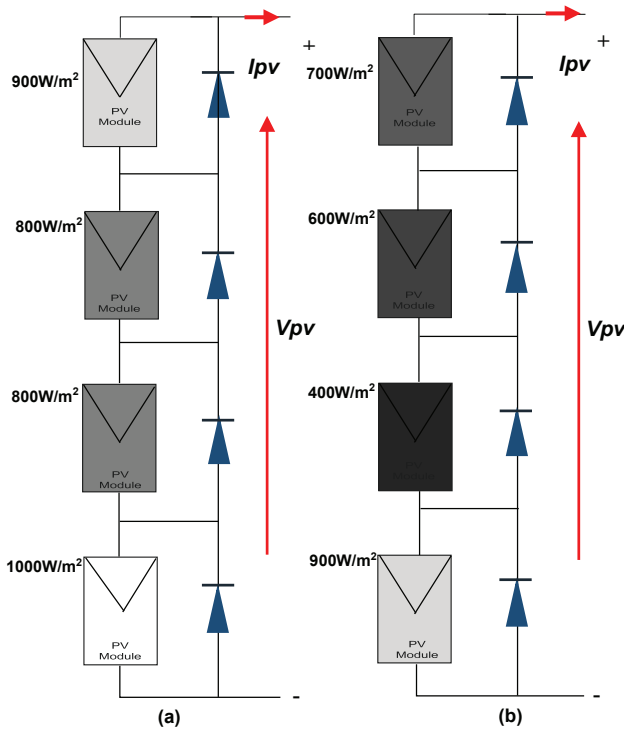
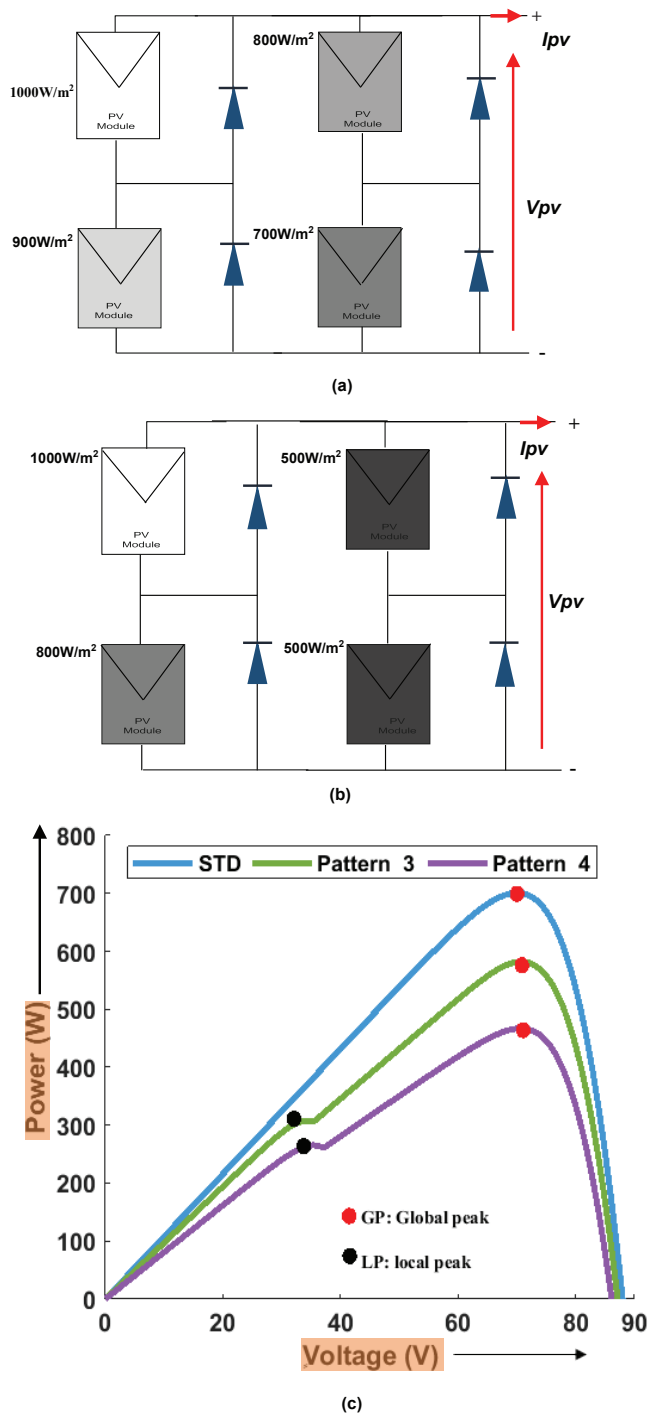


Fig. 2. Modules 4S configuration under different shading patterns. (a) Pattern 1. (b) Pattern 2. (c) P-V curves under PSCs.



**Fig. 3.** Modules 2S2P configuration under different shading patterns. (a) Pattern 3. (b) Pattern 4. (c) P –V curves under PSCs.

under the influence of different shading patterns. By contrast, Figure 3 shows a 2S2P configuration, an arrangement in which two series-connected modules are connected in parallel to two other series-connected modules.

This research employs MATLAB/SIMULINK simulations to explore and assess the effectiveness of PSO, GWO and HOA in achieving optimal performance in the presence of pro-posed particle shading.

## 4. Modeling Of Boost Converter

When the source is directly connected to a load, the PV module output power is infrequently maximum and optimal power is not obtained all the time. This issue is handled using a power converter interfaced between the solar system and the load. It transfers maximum power from solar panels to load (Sutikno et al., 2023). A promising solution is implementing a boost converter, illustrated as an equivalent circuit. It is made up of the following components: an input capacitor, an inductor, a resistance, a two-diode, a MOSFET and an output capacitor, as shown in Figure 4.

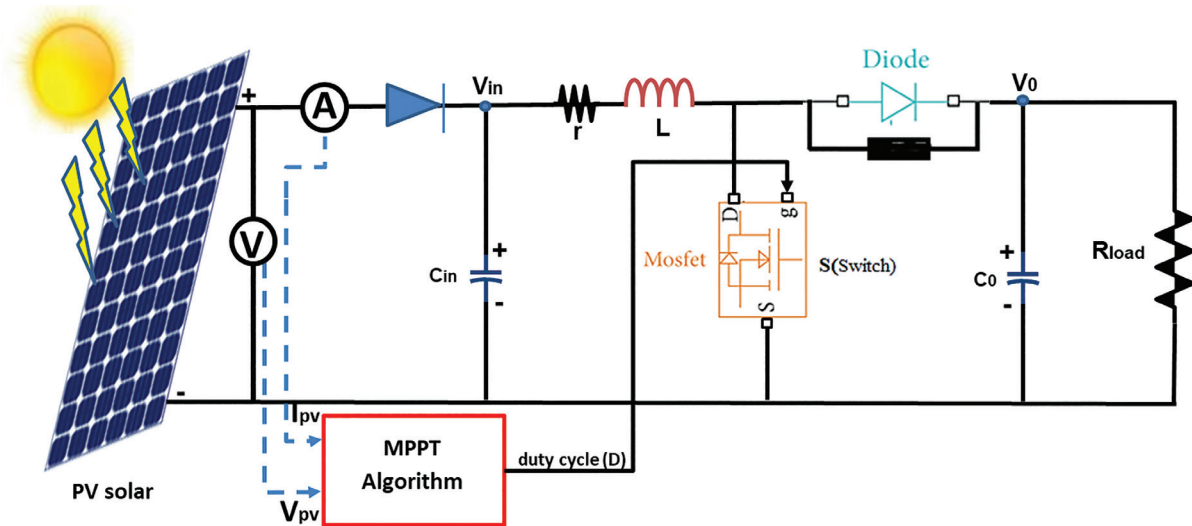


Fig. 4. Boost Converter equivalent circuit.

This boost converter can be characterised by two primary operational states: (1) Switch S ON and (2) Switch S OFF (Vangari et al., 2015). The mathematical expressions governing these states are presented below. ON state:

$$C_{in} \frac{dV_{in}}{dt} = i_{pv} - i \text{ and } L \frac{di}{dt} = v_{in} - ri - R_{on} i \quad (7)$$

- OFF state:

$$C_{in} \frac{dV_{in}}{dt} = i_{pv} - i \text{ and } L \frac{di}{dt} = v_{in} - ri - v_o - V_D \quad (8)$$

Where  $r$  is the inductor resistance,  $V_D$  is the diode forward voltage drop,  $i_{pv}$  is the current delivered by the solar array,  $R_{on}$  is the ON state resistance of the switch ( $R_{on} \approx 0$ ) and  $i$  is the inductor current. The electrical parameters of this module are listed in Table 2.

Table 2. Specification of the Boost Converter.

Parameters	Variable	Value
inductor	$L$	10 mH
resistance	$r$	0.05Ω
Input capacitor	$C_{in}$	330 μF
Output capacitor	$C_0$	1100μF
Load resistance	$R_{load}$	10Ω
Frequency	$f$	50KHZ

## 5. MPPT Algorithms

The MPPT control is a component of the PV system that enables monitoring of the generator's operation. It is utilised to identify the optimal power point for the system, considering load variations and weather conditions. The principle of its regulation is based on adjusting the duty cycle to the appropriate value in order to maximise the power output of a PV panel (Zafar et al., 2020).

### 5.1. Particle Swarm Optimization (PSO)

Kennedy and Eberhardt invented the PSO approach in 1995, which was inspired by the social behaviour of flocking birds and schooling fishes (Bettahaar et al., 2023). The approach is concerned with finding the best values for individual particles in a population.

The positions and velocities of each particle, as well as the global optimum position, are updated in each iteration of the PSO algorithm. To update the position and velocity of the particles in the population, Eqs (9) and (10) are applied as follows (Abo-Elyousr et al., 2019):

$$v_i(k+1) = \omega \times v_i(k) + c_1 \times r_1 \times (P_{best_i} - x_i(k)) + c_2 \times r_2 \times (G_{best} - x_i(k)) \quad (9)$$

$$x_i(k+1) = x_i(k) + v_i(k+1) \quad (10)$$

Where,  $i = 1, 2, \dots, N$  and  $N$  is the size of the population.  $x$  is the dimension of the search space.  $k$  represents the iteration number.  $c_1$  is the individual optimal coefficient,  $c_2$  is the individual global coefficient.  $\omega$  represents the weight of inertia.  $r_1$  and  $r_2$  are random numbers which are uniformly distributed in  $[0, 1]$ .  $P_{best}$  Represents the local optimum and  $G_{best}$  is a global best for the solution.

Throughout the iterative research process, a critical condition must be met, as expressed by the inequality:

$$P(X_i^{k+1}) > P(X_i^k) \quad (11)$$

Where  $P(X_i^k)$  and  $P(X_i^{k+1})$  are the PV power of the  $X_i$  particle at iterations  $K$  and  $K+1$ , respectively.

The search mechanism employed by the PSO-based tracker commences by initialising a random set of duty cycles, utilising four particles with initial values set at 0.1, 0.3, 0.6 and 0.9. Subsequently, each duty cycle is applied to the photovoltaic power system (PVPS), and the resulting system current and voltage are measured to estimate the power generated by the PVPS. This calculated power serves as the fitness function for each particle in the PSO algorithm.

After power estimation, a comparison is drawn between the newly calculated fitness value and the power corresponding to the personal best ( $P_{best}$ ) stored in the algorithm's history. If the newly estimated power surpasses the previous one, it is recognised as the new best fitness value for that particle. This iterative process repeats for all particles in the swarm.

Once all particles undergo evaluation, the old velocity and position for each particle are updated using Eqs (9) and (10). These equations govern how the positions and velocities of particles evolve based on their historical performance and the performance of their neighbors in the swarm.

The PSO-based tracker iterates through this process until a predetermined stopping criterion is met. The stopping criterion, a threshold fitness value in Eq. (11), signifies the completion of the optimisation process. Upon satisfaction of the stopping criterion, the PSO-based tracker concludes, furnishing the optimal duty cycle ( $D$  optimal) corresponding to the global power. Subsequently, the value of  $D$  optimal is transmitted to the pulse width modulation (PWM) box to regulate the operation of the boost converter.

### 5.2. Grey Wolf Optimization (GWO)

The GWO algorithm is based on the natural hierarchy of grey wolves and their hunting mechanism proposed by Mirjalili et al. (2014). For replicating the leadership hierarchy, grey wolves like alpha ( $\alpha$ ), beta ( $\beta$ ), delta ( $\delta$ ) and omega ( $\omega$ ) are used. We use the fittest solution as the alpha ( $\alpha$ ) to quantitatively simulate the social structure of wolves when building GWO. As a result, the second and third best solutions are referred to as beta ( $\beta$ ) and delta ( $\delta$ ). The remaining possible solutions are all considered as omega ( $\omega$ ), which is the worst. Grey wolves' hunting

habit is divided into three stages: searching, tracking and approaching prey, chasing down and encircling prey and attacking prey.

To implement the GWO-based MPPT, duty cycle  $d$  is defined as a grey wolf. Therefore, can be modified as follows:

$$\bar{D} = |\bar{C}\bar{X}_p(k) - \bar{X}_p(k)| \quad (12)$$

$$\bar{X}(k+1) = \bar{X}_p(k) - |\bar{A} \cdot \bar{D}| \quad (13)$$

Where  $K$  is the number of the iteration.  $D$ ,  $C$  and  $A$  denote coefficient vectors,  $X_p$  and  $X$  are the positions vectors of the prey and the grey wolf, respectively; and  $A$  and  $C$  are the coefficient vectors calculated by

$$\bar{A} = 2\bar{a} \cdot \bar{r}_1 - \bar{a} \quad (14)$$

$$\bar{C} = 2 \cdot \bar{r}_2 \quad (15)$$

Where components of an are linearly decreased from  $[2, 0]$  across iterations and  $r_1, r_2$  are random vectors in  $[0, 1]$ .

In the GWO-based search mechanism, the number of participating grey wolves symbolizes the duty cycles of the converter, and the MPP represents the prey being pursued:

$$D_i(k+1) = D_i(k) - A \times D \quad (16)$$

Thus, the fitness function of the GWO algorithm is formulated as:

$$P(D_i^k) > P(D_i^{k-1}) \quad (17)$$

The mathematical formulation of the equation is articulated as follows:  $P$  denotes power,  $D$  signifies duty cycle and  $i$  represents the individual grey wolves involved in the technique, where four grey wolves are employed with initial values set at 0.1, 0.3, 0.6, and 0.9. The parameter  $k$  denotes the number of iterations undertaken. The GWO-based MPPT algorithm's performance is influenced by several key parameters, including exploration and exploitation factors, population size and the maximum number of iterations.

Noteworthy attributes of the GWO algorithm encompass its simplicity in implementation, a minimal set of parameters requiring configuration and a high degree of tracking accuracy. However, it is imperative to acknowledge certain limitations, notably a relatively lower tracking speed, as elucidated by Mohanty et al. (2016).

### 5.3. Horse Herd Optimization Algorithm (HOA)

This research is based on the behavioural patterns of horses in their natural environment. The most typical behavioural patterns observed include grazing, hierarchy, sociability, imitation, defence mechanism and roaming (Miar Naeimi et al., 2021). The six common behaviours of horses of different ages provide inspiration for this approach. They exist at each step, according to the following equation:

$$P_m^{iter, age} = V_m^{iter, age} + P_m^{(iter-1), age}, \quad age = \alpha, \beta, \gamma, \delta \quad (18)$$

In this equation:

$P_m^{iter, age}$ : denotes the  $m$ th horse position.

$age$ : shows the range of each horse.

$iter$ : describes the current number of iterations.

$V_m^{iter, age}$ : illustrates the velocity of the vector of that horse

Horses exhibit a diverse range of behaviours throughout their lifespan. On average, horses live for approximately 25–30 years. To categorise horses based on age, we use symbols to represent different age groups:  $\delta$  for horses aged 0–5,  $\gamma$  for horses aged 5–10,  $\beta$  for horses aged 10–15 and  $\alpha$  for horses older than 15 years. Determining the

age of horses involves a thorough matrix of questions and answers. This matrix can be organised in a way that the best replies are ranked at the top. We then select the top 10% of horses from this ordered matrix as  $\alpha$  horse, representing those older than 15 years. The subsequent 20% of horses form the  $\beta$  group, encompassing horses aged 10–15 years. The remaining horses are divided into the  $\gamma$  and  $\delta$  groups, accounting for 30% and 40% of the population, respectively.

To calculate the velocity vector, we employ quantitative methods that imitate the six actions performed by each group of horses. These methods allow us to analyse and measure the movement and behaviour patterns specific to each age group (Elmanakhly et al., 2022):

$$Vel_m^{iter,\alpha} = Gra_m^{iter,\alpha} + DefMec_m^{iter,\alpha} \quad (19)$$

$$Vel_m^{iter,\beta} = Gra_m^{iter,\beta} + H_m^{iter,\beta} + Soc_m^{iter,\beta} + DefMec_m^{iter,\beta} \quad (20)$$

$$Vel_m^{iter,\gamma} = Gra_m^{iter,\gamma} + H_m^{iter,\gamma} + Soc_m^{iter,\gamma} + Imt_m^{iter,\gamma} + Ro_m^{iter,\gamma} + DefMec_m^{iter,\gamma} \quad (21)$$

$$Vel_m^{iter,\delta} = Gra_m^{iter,\delta} + I_m^{iter,\delta} + Ro_m^{iter,\delta} \quad (22)$$

The following systematic tracking mechanism of HOA is illustrated in Figure 5 (Sanam Kouser et al., 2022):

### 1. Gazing

Horses spend 16-20 hours per day staring at a field. The following is a mathematical interpretation of staring.

$$\begin{aligned} G_m^{iter,A} &= g_{iter}(\mu + \rho l) [X_m^{iter-1}], \quad A = \alpha, \beta, \delta, \gamma \\ g_m^{iter,A} &= g_m^{(itr-1),A} \times \omega_g \end{aligned} \quad (23)$$

Where  $G_m^{ite,A}$  indicates the motion parameter of  $l^{th}$  horse. The value of 1 can be taken as 0.95 and  $\mu$  can be taken as 1.05.  $g$ , the coefficient, can be taken as 1.5 for horses of all ages.

### 2. Hierarchy

Horses spend their entire lives following a leader. According to the law of hierarchy, an adult stallion or mare in a herd of wild horses is also accountable for. In this scenario, the coefficient  $h$  represents the herd's predisposition to follow the most experienced and strongest horse. According to studies, horses followed the law of hierarchy throughout the medieval times, and the following equations can be used to define the Hierarchy layer:

$$\begin{aligned} H_m^{iter,A} &= h_m^{iter,A} [X_*^{ite-1} - X_m^{iter-1}], \quad A = \alpha, \beta, \gamma \\ h_m^{iter,A} &= h_m^{(itr-1),A} \times \omega_h \end{aligned} \quad (24)$$

Here,  $H_m^{itr,A}$  indicates the effects of the best horse location, on velocity parameter, and  $X_*^{(itr-1)}$  indicates the location of the best horse.

### 3. Sociability

Horses are gregarious creatures, thus they sometimes coexist with other animals. It is better for the horse's security to live in a herd. Loneliness bothers horses. They enjoy being near other animals such as cattle and sheep. This conduct, as indicated by a factor  $s$ , suggests migration toward an average location of other horses. The following equation represents horse sociability:

$$\begin{aligned} S_m^{iter,A} &= s_m^{iter,A} \left[ \left( \frac{1}{N} \sum_{j=1}^N X_j^{iter-1} \right) - X_m^{itr-1} \right], \quad A = \beta, \gamma \\ s_m^{iter,A} &= s_m^{(itr-1),A} \times \omega_s \end{aligned} \quad (25)$$

Here,  $S_m^{iter,A}$  is Social motion vector of  $i^{th}$  horse,  $S_m^{ther,A}$  is concerned horses orientation towards the herd in  $iter^{th}$  iteration, and  $N$  is the total number of horses.

#### 4. Imitation

Horses imitate one another. They learn each other's' good and bad habits and discover their ideal grazing spot. In this algorithm, factor  $i$  represents the imitation behaviour. Young horses strive to imitate one another. They continue to do so until they reach full maturity:

$$I_m^{ite,A} = i_m^{iter,A} \left[ \left( \frac{1}{\rho N} \sum_{j=1}^{\rho N} X_j^{iter-1} \right) - X^{iter-1} \right], A = \gamma \quad (26)$$

$$i_m^{iter,A} = i_m^{(iter-1),A} \times \omega_i$$

Here,  $I_m^{iter,A}$  is the motion vector of  $i^{th}$  horse towards the average best horse with  $X$  location,  $\rho N$  is the number of horses with best locations,  $\rho$  is, usually, 10% of the horses,  $\omega_i$  is the reduction factor per cycle.

#### 5. Defense Mechanism

It is well known that horses defend themselves by flight or fight reaction. They attempt to flee first and buck when trapped. Horses compete with one another for food and water. They also have to contend with an unfriendly or hazardous environment. In the HOA, horses' protection strategy includes running away from horses that exhibit unacceptable behaviour. The defence mechanism is active throughout a horse's life. The defence mechanism of horses is indicating by following equations:

$$D_m^{iter,A} = -d_m^{ite,A} \left[ \left( \frac{1}{qN} \sum_{j=1}^{qN} X_j^{(iter-1)} \right) - X^{(iter-1)} \right], A = \alpha, \beta, \gamma \quad (27)$$

$$d_m^{iter,A} = d_m^{(iter-1),A} \times \omega_d$$

Where,  $D_m^{iter,A}$  is the escape vector of  $i^{th}$  horse from the average of some horses with worst locations which are shown by  $X$  vector,  $qN$  is the Number of horses with worst location,  $q$  is 20% of the total horses,  $\omega_d$  is the reduction factor per cycle for  $d_{iter}$ .

#### 6. Roam

It is a fact that horses roam outside in search of food. A horse may suddenly go somewhere to graze. Horses are usually very curious and visit new places to discover new pastures or to know their neighbourhood well. The roaming in a horse is usually found in young ages and gradually disappears with attaining maturity. The equations describing this stage are as follows:

$$R_m^{iter,A} = r_m^{itter,A} \rho X^{(iter-1)}, A = \gamma, \delta \quad (28)$$

$$r_m^{iter,A} = r_m^{(iter-1),A} \times \omega_r$$

Here,  $R_m^{iter,A}$  is the random velocity vector of  $i^{th}$  horse for a local search and escape for velocities of the horses under  $\delta, \gamma, \beta$  and  $\alpha$  categories respectively.

Equations (29)-(31) give the velocities of the horses under  $\delta, \gamma, \beta$  and  $\alpha$  categories respectively.

Velocity of  $\delta$  horses at the age of 0 – 5 years:

$$Vel_m^{iter,\delta} = \left[ w_g \times g_m^{(iter-1),\delta} (low + r*upp) \left[ P_m^{(iter-1)} \right] \right] + im_m^{(-1+ iter),\delta} \times \omega_{im} \times \left[ \left( \frac{1}{\rho N} \sum_{j=1}^{\rho N} P_j^{(-1+ iter)} \right) - P^{(-1+ iter)} \right] \quad (29)$$

$$+ ro_m^{(-1+ iter),\delta} \times \omega_{ro} \times \delta P^{(-1+ iter)}$$

Velocity of  $\gamma$  horses at the age of 5-10 years:

$$\begin{aligned}
 Vel_m^{\text{ter}, \gamma} = & \left[ w_g \times g_m^{(\text{tter}-1), \gamma} (\text{low} + r^* \text{upp}) \left[ P_m^{(\text{ther}-1)} \right] \right] + h_m^{(-1+ \text{tter}), \gamma} \times w_h \times \left[ P_{\text{lbh}}^{(\text{ther}-1)} - P_m^{(\text{tter}-1)} \right] \\
 & + soc_m^{(-1+ \text{tter}), \gamma} \times \omega_{\text{soc}} \times \left[ \left( \frac{1}{N} \sum_{j=1}^N P_j^{(-1+ \text{tter})} \right) - P_m^{(-1+ \text{tter})} \right] + im_m^{(-1+ \text{tter}), \gamma} \times \omega_m \times \left[ \left( \frac{1}{pN} \sum_{j=1}^{pN} P_j^{(-1+ \text{tter})} \right) - P^{(-1+ \text{tter})} \right] \\
 & + im_m^{(-1+ \text{tter}), \gamma} \times \omega_m \times \left[ \left( \frac{1}{pN} \sum_{j=1}^{pN} P_j^{(-1+ \text{tter})} \right) - P^{(-1+ \text{tter})} \right] + ro_m^{(-1+ \text{tter}) \text{ age}} \times \omega_{ro} \times \partial P^{(-1+ \text{itter})}
 \end{aligned} \quad (30)$$

Velocity of  $\beta$  horses at the age of 10 – 15 years:

$$\begin{aligned}
 Vel_m^{\text{fler}, \beta} = & \left[ w_g \times g_m^{(\text{tter}-1), \beta} (\text{low} + r^* \text{upp}) \left[ P_m^{(\text{tter}-1)} \right] \right] + h_m^{(-1+ \text{tter}), \beta} \times w_h \times \left[ P_{\text{lbh}}^{(\text{ther}-1)} - P_m^{(\text{tter}-1)} \right] \\
 & + soc_m^{(-1+ \text{tter}), \beta} \times \omega_{\text{soc}} \times \left[ \left( \frac{1}{N} \sum_{j=1}^N P_j^{(-1+ \text{fler})} \right) - P_m^{(-1+ \text{fler})} \right] - \text{defmec}_m^{(-1+ \text{tter}), \beta} \times \omega_{\text{defmec}} \\
 & \times \left[ \left( \frac{1}{qN} \sum_{j=1}^{qN} P_j^{(-1+ \text{titer})} \right) - P^{(-1+ \text{tter})} \right]
 \end{aligned} \quad (31)$$

The tracking mechanism HOA based MPPT (Sarwar et al., 2020):

Within the software block, the HOA is applied utilising two inputs: the continuous readings of current and voltage obtained from the PV module. Subsequently, the algorithm processes these data to compute the duty cycle value, which signifies the optimal point for achieving maximum power in the system. This duty cycle is then integrated into the control mechanism to facilitate efficient power extraction.

The initiation of the proposed HOA control involves initialising various variables, including duty cycle (u), current duty cycle (dcurrent), best position of the horse (pbest), calculated power (p), velocity (v), counter, global best duty cycle (gbest), worst duty cycle (bbest), position of the horse (CC), mean duty cycle (mean\_d) and the number of horses (nHorse). These variables are assigned specific initial values to establish the baseline conditions for the optimization process.

The subsequent steps involve the calculation of fitness values (Power = Current × Voltage) based on the initial conditions. The velocities and duty cycles of the horses are updated accordingly. The horses are categorised based on their fitness, and specific parameters (alphas, betas, gammas, deltas) are assigned to influence their behaviour, encompassing grazing, defence mechanisms, hierarchy, sociability, imitation, random wandering and curiosity.

Furthermore, the algorithm calculates the position of each horse (CC) based on its fitness value. Depending on the range of CC relative to the total number of horses (nh), distinct algorithms are employed to update the velocity and position. These updates, influenced by parameters such as alpha, beta, gamma and delta, aim to guide the horses towards optimal frequencies, thereby maximising power output.

In the final step of the HOA, specific conditions are evaluated, and the optimal horse position (frequency) is retained upon achieving maximum power. This iterative process involves continuous updates to the velocities and positions of the horses until a predetermined stopping criterion is met, indicated by the counter reaching a specified limit. In such instances, the algorithm ensures the preservation of the best horse position, thereby maintaining the duty cycle at the global best duty cycle (gbest). This cycle persists until a predefined condition is satisfied, such as when the iteration counter reaches a limit of (counter < 300).

Figure 5 presents a flowchart that systematically illustrates the control process, enhancing the understanding of the research procedure concerning the optimal duty cycle within the HOA.

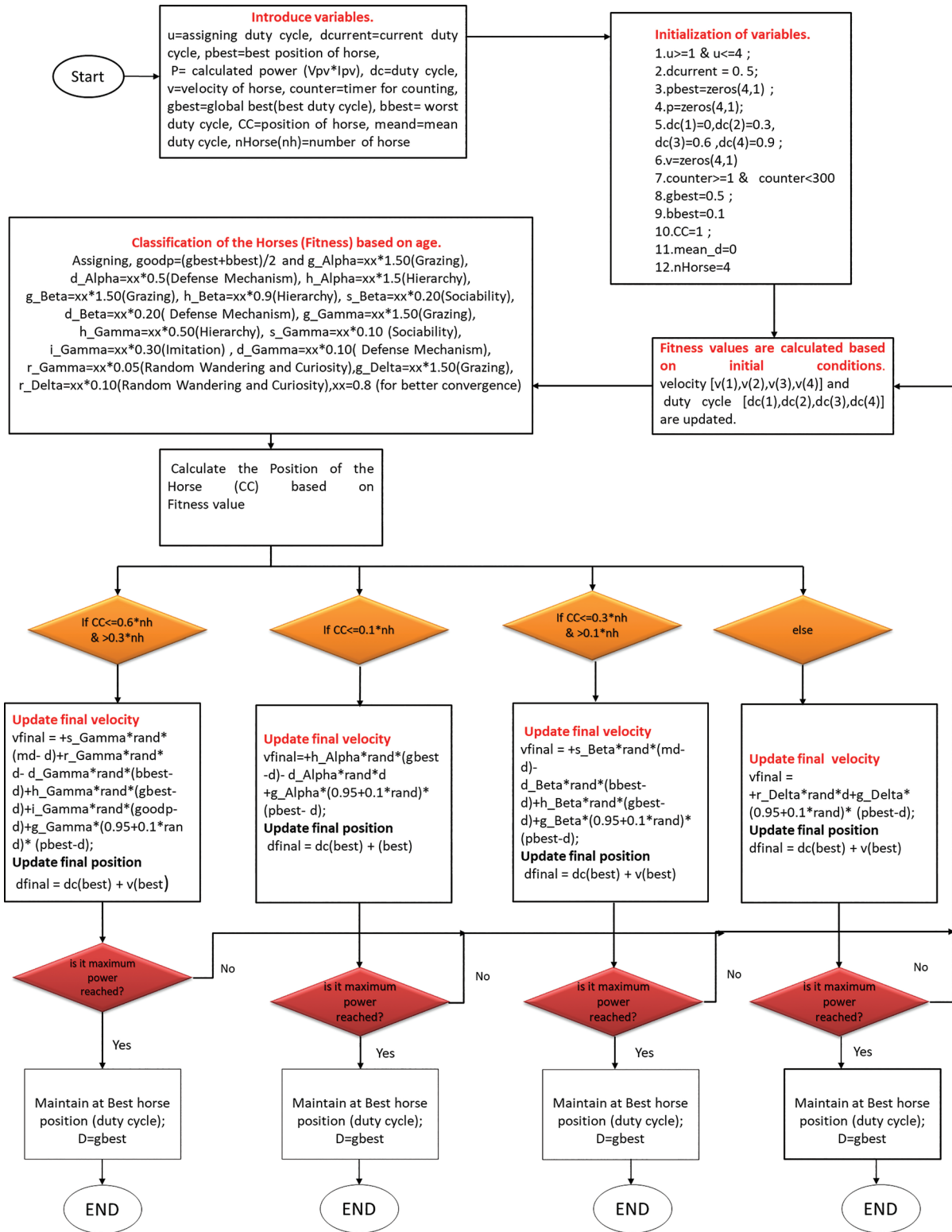


Fig. 5. Flowchart of the HOA.

## 6. Simulation and Results

In the framework of four randomly partial shading scenarios, this study investigates the outcomes attained by applying three distinct MPPT techniques: PSO, GWO and HOA, as shown in Figure 6. MATLAB SIMULINK® software version 2022a is used during the experimentation phase on a PC with an Intel i5 processor and 8GB RAM. The adoption of MATLAB/SIMULINK is especially important, since it is a wonderful platform for learning and research and is widely recognised and used in companies, research centres and academic institutions. The MATLAB software's solver setup was modified to execute the algorithms at a fixed step.

The simulation results are illustrated in Figures 7 and 8.

In Pattern 1, the PV module's serial assembly (4S) undergoes fluctuating levels of irradiation, specifically 900 W/m<sup>2</sup>, 800 W/m<sup>2</sup>, 800 W/m<sup>2</sup> and 1,000 W/m<sup>2</sup>. This information is visually represented in Figure 2a. Notably, the PV characteristic curve in Figure 2c illustrates the generation of three distinct peaks: two LMPP and one GMPP at 588.8 W.

Furthermore, the comparative performance of the HOA method is demonstrated in Figure 7a. Remarkably, this method swiftly attains a GMPP at 588.5 W within a mere 0.15 s. Notably, the attainment is achieved without encountering any persistent oscillations in the steady state.

By contrast, the behaviours of the PSO and GWO methods display subtle distinctions. The PSO method achieves a power output of 569.6 W within approximately 0.76 s, while the GWO method reaches 572.02 W in about 0.32 s. However, both methods are accompanied by minor steady-state oscillations that result in a marginal power loss. Despite their slight nature, these oscillations contribute to a reduction in overall power efficiency.

In Pattern 2, variable solar irradiation intensities were applied to the serial PV module (4S) assemblies. This situation is an example of extreme shadowing, because there is a significant variation in the sun radiation intensities: 700 W/m<sup>2</sup>, 600 W/m<sup>2</sup>, 900 W/m<sup>2</sup> and 900 W/m<sup>2</sup>. This condition resulted in the emergence of four distinctive peaks on the P–V curve, as clearly depicted in Figure 2c. Notably, the third peak stands out as a global maximum, reaching a power output of 339.9 W.

As shown in Figure 7b, the performance of the HOA method is evident. Impressively, this method swiftly converged to a GMPP of 339.1 W within a mere 0.14 s. In comparison, the PSO method achieved a power output of 320.3 W after a duration of 0.78 s, while the GWO method reached 330 W within 0.33 s. It is noteworthy that the HOA is better than both the PSO and GWO methods.

In Pattern 3, the configuration involves a parallel installation of PV modules in a 2P2S (2 Parallel 2 Series) arrangement, specifically subjected to shading conditions of 1,000 W/m<sup>2</sup> and 800 W/m<sup>2</sup> for the upper PV, and 900 W/m<sup>2</sup> and 700 W/m<sup>2</sup> for the lower PV, as depicted in Figure 3a. Notably, the resulting characteristic curve, shown in

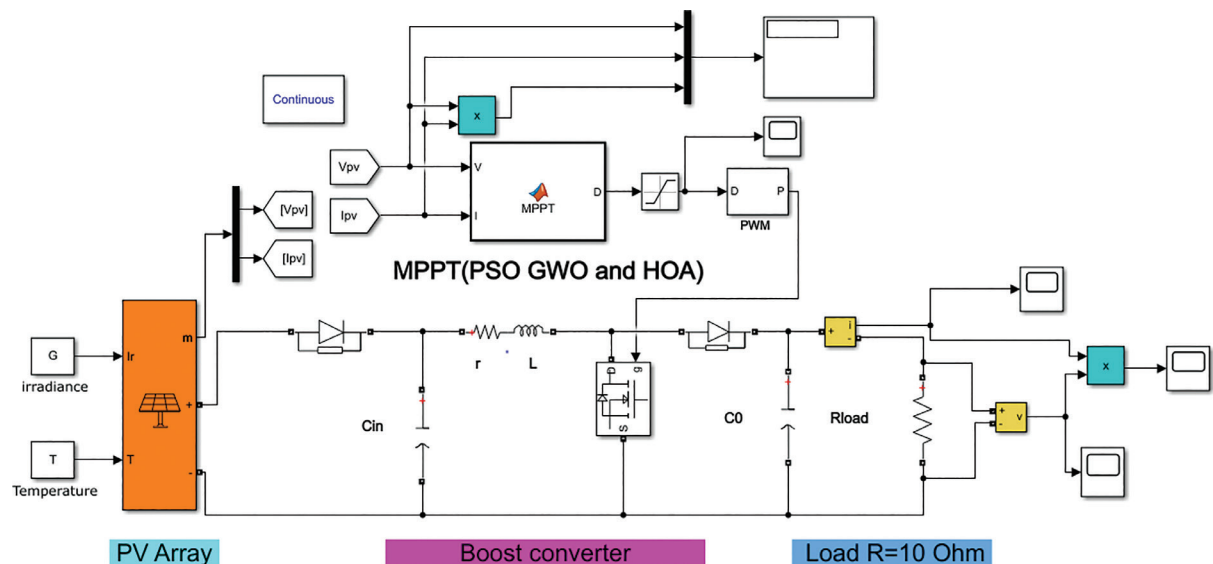
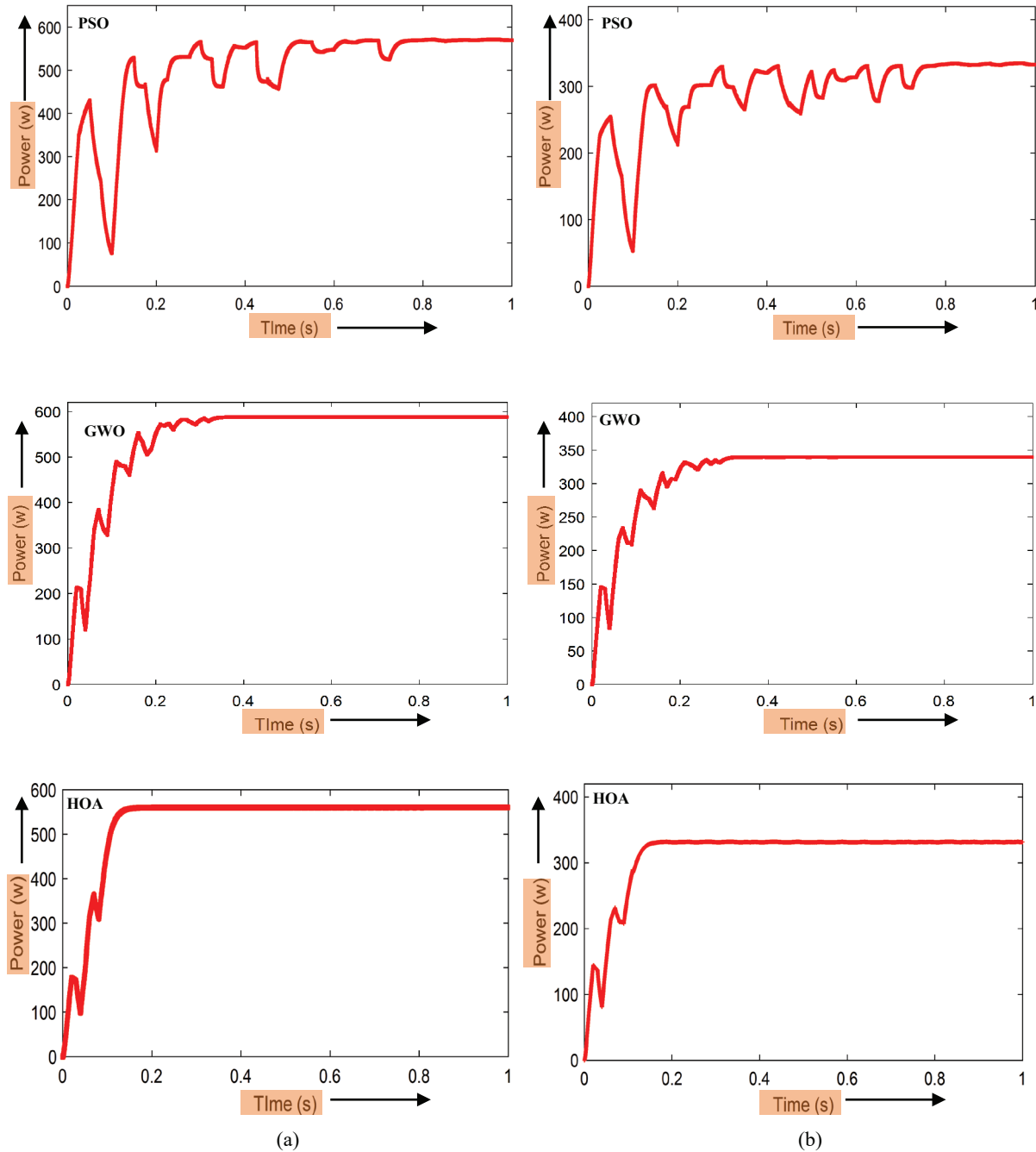


Fig. 6. Simulink model of standalone PV system with MPPT controller under patterns (1)–(4).



**Fig. 7.** Tracking process of GMPP on (a) Pattern 1, (b) Pattern 2.

Figure 3c, exhibits a single global peak, denoted as GMPP, with a value of 143.2 W, alongside another local peak, LMPP. Interestingly the HOA technique shows effectiveness in this situation. It quickly reaches within just 0.08 s a GMPP of 582.2 W. In contrast, the GWO approach needs 0.36 s longer to get a GMPP of 571.3 W. Additionally, the PSO approach converges in 0.89 s and reaches a peak power output GMPP of 561.5 W, as shown in Figure 8a.

In Pattern 4, the configuration entails the installation of PV modules in parallel in a 2P2S (2 Parallel 2 Series) configuration under shading circumstances of 1,000 W/m<sup>2</sup> and 800 W/m<sup>2</sup> for the top PV, and 500 W/m<sup>2</sup> and 500 W/m<sup>2</sup> for the bottom PV, as shown graphically in Figure 3b. The resulting characteristic curve, shown in

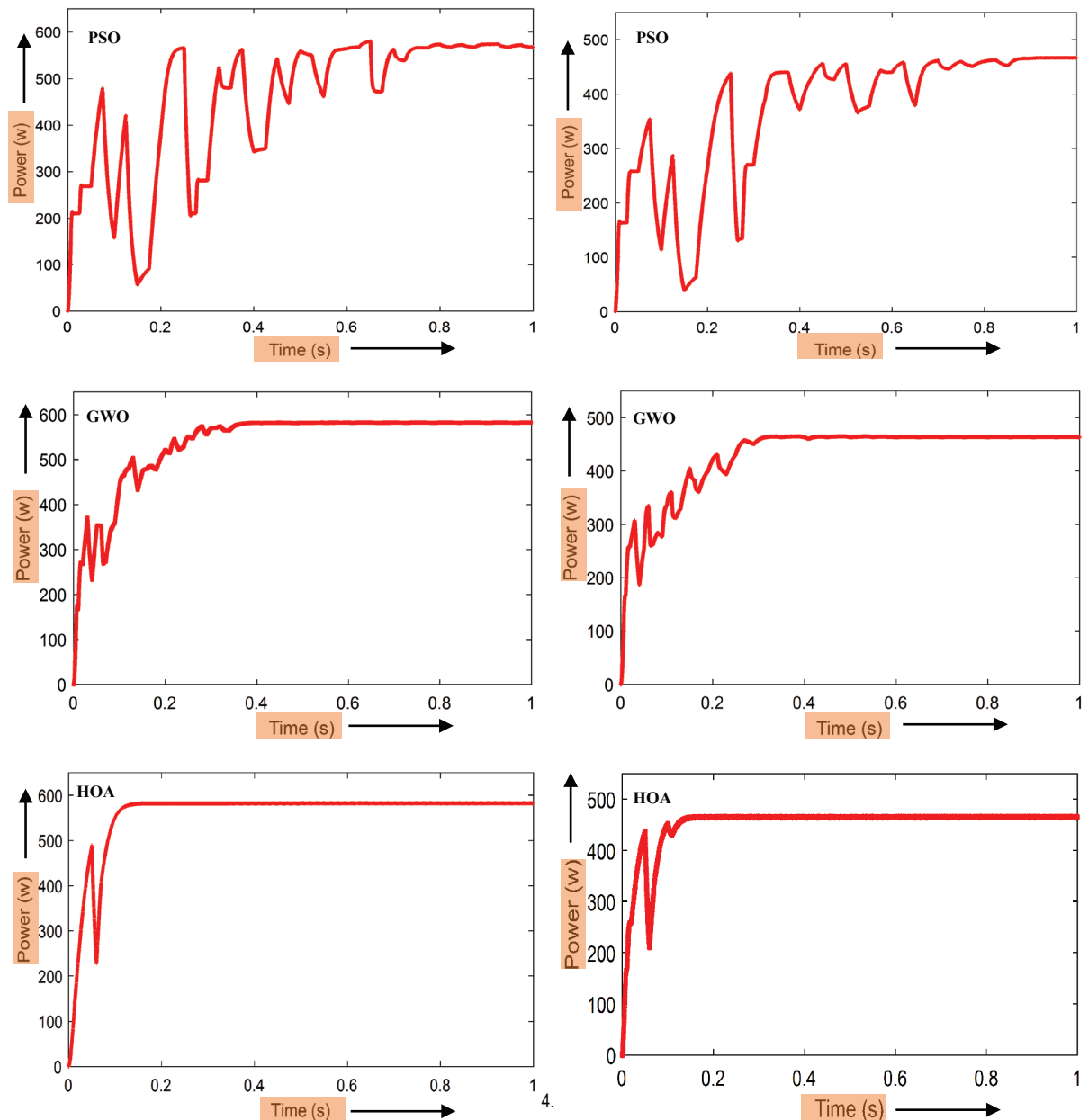


**Fig. 8.** Tracking process of GMPP on (a) Pattern 3, (b) Pattern 4.

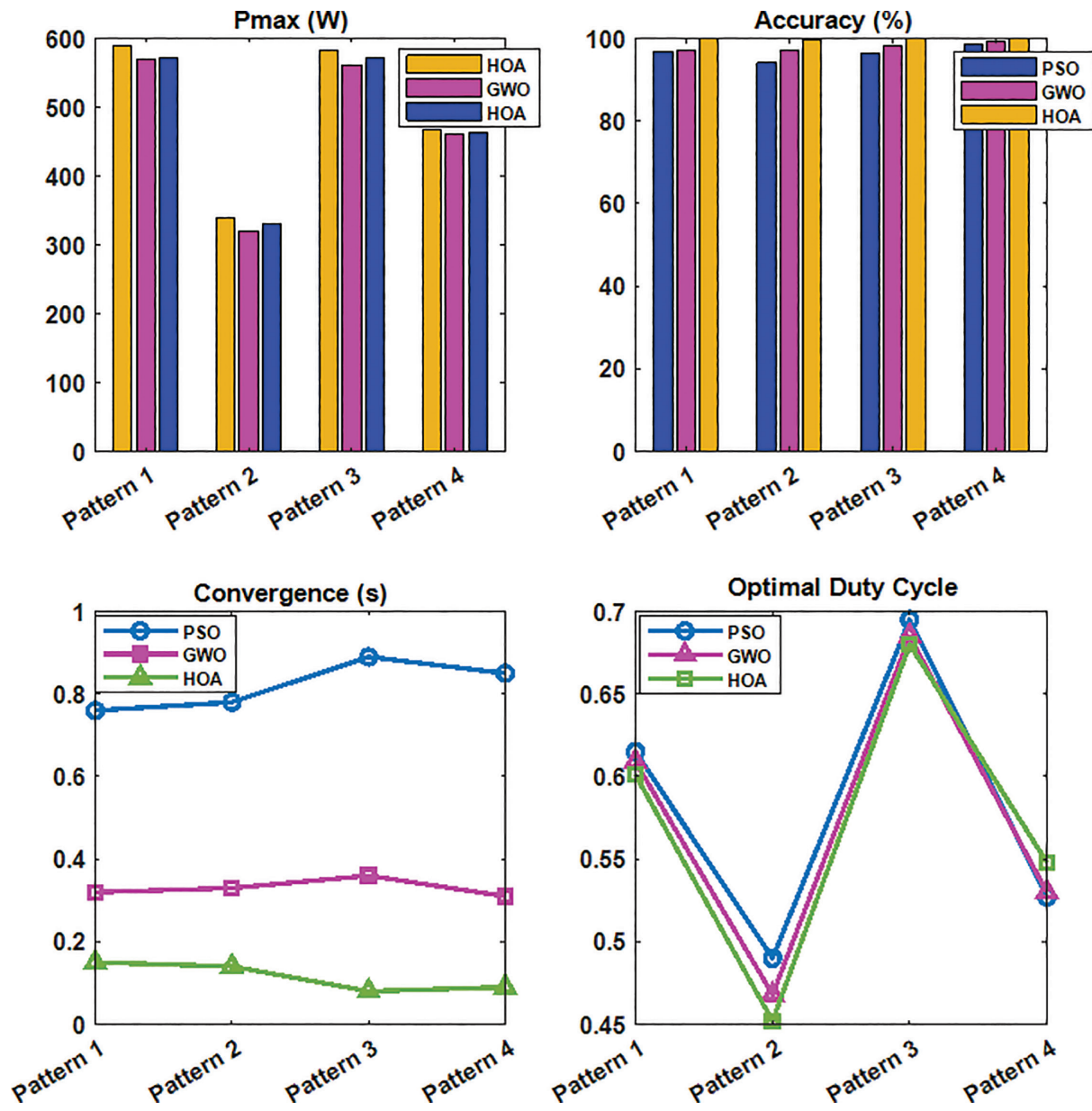
Figure 3c, notably exhibits a single notable peak known as GMPP with a value of 467.1 W, and an accompanying local peak LMPP.

As shown in Figure 8b, the (HOA) technique demonstrates its outstanding efficacy in this specific case. It exhibits quick convergence by achieving a GMPP of 467.05 W in an astonishingly short time (0.09 s). The GWO method converges quickly (0.31 s) and with a maximum power output of 464 W. Similar results are obtained using the PSO approach, however, it takes a little longer (0.85 s) to reach convergence. Delivering outcomes are consistently on par with or superior to those reached using GWO and PSO methods.

Based on the simulation results, an accurate quantitative comparison between PSO, GWO and HOA methods is illustrated in Table 3, by considering the following performance criteria: efficiency, convergence time and extracted PV power.

**Table 3.** Comparison Result of PSO, GWO and HOA Method.

Shading Pattern	Pmax (W)				Accuracy (%)			Convergence (second)		
	Target	PSO	GWO	HOA	PSO	GWO	HOA	PSO	GWO	HOA
Pattern 1	588.8	569.6	572.02	588.5	96.73	97.15	99.940	0.76	0.32	0.15
Pattern 2	339.9	320.3	330	339.1	94.20	97.08	99.76	0.78	0.33	0.14
Pattern 3	582.2	561.5	571.3	581.4	96.27	98.12	99.86	0.89	0.36	0.08
Pattern 4	467.1	461.2	464	467.05	98.73	99.33	99.98	0.85	0.31	0.09

**Fig. 9.** Quantitative comparison between the performances of PSO, GWO and HOA methods for different Shading Pattern.

The results shown in Table 3 and Figure 9 make it clear that the HOA performs better than the other suggested approaches in a variety of ways. Notably, HOA excels in tracking accuracy convergence speed, and the ability to precisely calculate the ideal duty cycle.

The data collected during the experimental phase enabled calculation of the efficiency percentage (%) for each method, as outlined in Table 3. It is apparent from the table that the accuracy (%) ( $=P_{max}(W) \text{ for each technique} \times 100 / P_{max} \text{ Target}(W)$ ) achieved by the HOA method is notably higher than that of the other techniques.

These findings emphasise the efficacy and prowess of the HOA in optimising the MPPT process for PV systems. HOA's superior accuracy convergence speed, and efficiency percentage underscore its potential as a compelling choice for optimising power generation and overcoming shading challenges in PV applications.

## 7. Conclusion

In conclusion, this study has highlighted the efficiency, adaptability and robustness of intelligent controller techniques, leading to near-optimal results in the context of solar PV energy systems. Specifically, the research focused on a standalone solar PV system operating under partial shading conditions for maximum power tracking with MPPT. Among the three algorithms evaluated for GMPP tracking, the HOA demonstrated exceptional performance; its outstanding speed, efficiency and convergence in locating the GMPP set it apart from the previous algorithms. Across all scenarios, the HOA approach consistently outperformed the other two MPPT tracking methods, particularly when faced with increased shading on the panels. For instance, in the fourth pattern, HOA achieved an impressive 99.98% efficiency and attained the GMPP 45% faster than the comparative approaches (GWO and PSO).

Overall, this research provides compelling evidence for the superiority of the HOA algorithm in maximising power generation from solar PV systems, especially under varying shading conditions. These findings contribute significantly to the advancement of more efficient and adaptive solar energy systems, thereby promoting the widespread adoption of renewable energy technologies.

## References

- Abo-Elyousr, F. K., Abdelshafy, A. M. and Abdelaziz, A. Y. (2019). MPPT-based particle swarm and cuckoo search algorithms for PV systems. In: *Modern Maximum Power Point Tracking Techniques for Photovoltaic Energy Systems*, pp. 379–400. doi: 10.1007/978-3-030-05578-314.
- Ahmed, J. and Salam, Z. (2015). A Critical Evaluation on Maximum Power Point Tracking Methods for Partial Shading in PV Systems. *Renewable and Sustainable Energy Reviews*, 47, pp. 933–953. doi: 10.1016/j.rser.2015.03.080.
- Ahmad, R., Murtaza, A. F., and Sher, H. A. (2019). Power tracking techniques for efficient operation of photovoltaic array in solar applications – a review, *Renewable and Sustainable Energy Reviews*, 101, 82–102. doi :10.1016/j.rser.2018.10.015
- Baba, A. O., Liu, G. and Chen, X. (2020). Classification and Evaluation Review of Maximum Power Point Tracking Methods. *Sustainable Futures*, 2, p. 100020. doi: 10.1016/j.sftr.2020.100020.
- Bettahar, F., Sabrina, A. and Achour, B. (2023). Enhancing PV Systems with Intelligent MPPT and Improved Control Strategy of Z-Source Inverter. *Power Electronics and Drives*, 9(1), pp. 1–20. doi: 10.2478/pead-2024-0001.
- Bhukya, M. N. and Kota, V. R. (2018). A Novel P&OT-Neville's Interpolation MPPT Scheme for Maximum PV System Energy Extraction. *International Journal of Renewable Energy Development*, 7(3), pp. 251–260. doi: 10.14710/ijred.7.3.251-260.
- Bollipo, R. B., Mikkili, S. and Bonthagorla, P. K. (2020). Critical Review on PV MPPT Techniques: Classical, Intelligent and Optimisation. *IET Renewable Power Generation*, 14, pp. 1433–1452. doi: 10.1049/iet-rpg.2019.1163.
- Chauhan, U., Rani, A., Kumar, B. and Singh, V. (2019). A Multi Verse Optimization based MPPT Controller for Drift Avoidance in Solar System. *Intelligent & Fuzzy Systems*, 36(3), pp. 2175–2184. doi: 10.3233/JIFS-169929.
- Chellal, M., Guimarães, T. F. and Leite, V. (2021). Experimental Evaluation of MPPT algorithms: A Comparative Study. *International Journal of Renewable Energy Research*, 11(1). doi: 10.20508/ijrer.v11i1.11797.g8164.

- Elmanakhly, D. A., Saleh, M., Rashed, E. A. and Abdel-Basset, M. (2022). BinHOA: Efficient Binary Horse Herd Optimization Method for Feature Selection: Analysis and Validations. *IEEE Access*, 10, pp. 26795–26816. doi: 10.1109/access.2022.3156593.
- Hanafiah, S., Ayad, A., Hehn, A. and Kennel, R. (2017). "A hybrid MPPT for quasi-Z-source inverters in PV applications under partial shading condition," *2017 11th IEEE International Conference on Compatibility, Power Electronics and Power Engineering (CPE-POWERENG)*, Cadiz, Spain, 2017, pp. 418-423, doi: 10.1109/CPE.2017.7915208.
- Hota, S., Sahu, M. K. and Malla, J. M. R. (2017). A Standalone PV System with a Hybrid P&O MPPT Optimization Technique, Engineering. *Technology & Applied Science Research*, 7(6), pp. 2109–2112. doi: 10.48084/etasr.1374.
- Jately, V., Azzopardi, B., Joshi, J., Sharma, A. and Arora, S. (2021). Experimental Analysis of Hill-Climbing MPPT Algorithms under Low Irradiance Levels. *Renewable and Sustainable Energy Reviews*, 150, p. 111467. doi: 10.1016/j.rser.2021.111467.
- Khan, K., Rashid, S., Mansoor, M., Khan, A., Raza, H., Zafar, M. H. and Akhtar, N. (2023). Data-Driven Green Energy Extraction: Machine Learning-Based MPPT Control with Efficient Fault Detection Method for the Hybrid PV-TEG System. *Energy Reports*, 9, pp. 3604–3623. doi: 10.1016/j.egyr.2023.02.047.
- Kouser, S., Dheep, R. and Bansal, R. C. (2022). Horse herd optimization MPPT for grid connected PV system under partial shading conditions. In: *IEEE 10th Power India International Conference (PIICON)*, New Delhi, India, pp. 1–6.
- Krishna, K. S. and Kumar, K. S. (2015). A Review on Hybrid Energy Systems. *Renewable and Sustainable Energy Reviews*, 52, pp. 907–916. doi: 10.1016/j.rser.2015.070187.
- Kumar, C. S. and Rao, R. S. (2016). A Novel Global MPP Tracking of Photovoltaic System based on Whale Optimization Algorithm. *International Journal of Renewable Energy Development*, 5(3), pp. 225–232. doi: 10.14710/ijred.5.3.225-232.
- Li, D., Zhou, H., Zhou, Y., Rao, Y. and Yao, W. (2023). Atom Search Optimization-based PV Array Reconfiguration Technique under Partial Shading Condition. *International Transactions on Electrical Energy Systems*, pp. 1–15. doi: 10.1155/2023/8685976.
- Li, H., Yang, D., Su, W., Lu, J. and Yu, X. (2019). An Overall Distribution Particle Swarm Optimization MPPT Algorithm for Photovoltaic System under Partial Shading. *IEEE Transactions on Industrial Electronics*, 66(1), pp. 265–275. doi: 10.1109/tie.2018.2829668.
- Memaya, M. B., Moorthy, C. B., Tahiliani, S. and Sreeni, S. (2019). Machine Learning Based Maximum Power Point Tracking in Solar Energy Conversion Systems. *International Journal of Smart Grid and Clean Energy*, 8(6), pp. 662–669. doi: 10.12720/sgce.8.6.662-669.
- Miar Naeimi, F., Azizyan, G. and Rashki, M. (2021). Horse Herd Optimization Algorithm: A Nature-Inspired Algorithm for High-Dimensional Optimization Problems. *Knowledge Based Systems*, 213, p. 106711. doi: 10.1016/j.knosys.2020.106711.
- Mirjalili, S., Mirjalili, S.M. and Lewis, A. (2014). A Grey Wolf Optimizer. *Advances in Engineering Software*, 69, pp. 46–61. doi: 10.1016/j.advengsoft.2013.12.007.
- Mohanty, S., Subudhi, B. and Ray, P. K. (2016). A New MPPT Design Using Grey Wolf Optimization Technique for Photovoltaic System under Partial Shading Conditions. *IEEE Transactions on Sustainable Energy*, 7(1), pp. 181–188. doi: 10.1109/TSTE.2015.2482120.
- Motahhir, S., El Hammoumi, A. and El Ghzizal, A. (2018). Photovoltaic System with Quantitative Comparative between an Improved MPPT and Existing INC and P&O Methods Under Fast Varying of Solar Irradiation. *Energy Reports*, 4, pp. 341–350. doi: 10.1016/j.egyr.2018.04.003.
- Naick, B. K., Chatterjee, T. K. and Chatterjee, K. (2017). Performance Analysis of Maximum Power Point Tracking Algorithms under Varying Irradiation. *International Journal of Renewable Energy Development*, 6(1), pp. 65–74. doi: 10.14710/ijred.6.1.65-74.
- Nassef, A. M., Abdelkareem, M. A., Maghrabie, H. M. and Baroutaji, A. (2023). Review of Metaheuristic Optimization Algorithms for Power Systems Problems. *Sustainability*, 15(12), p. 9434. doi: 10.3390/su15129434.
- Peng, B. R., Ho, K. C. and Liu, Y. H. (2018). A Novel and Fast MPPT Method Suitable for Both Fast Changing and Partially Shaded Conditions. *IEEE Transactions on Industrial Electronics*, 65(4), pp. 3240–3251. doi: 10.1109/tie.2017.2736484.
- Phan, B. C., Lai, Y.-C. and Lin, C. E. (2020). A Deep Reinforcement Learning-Based MPPT Control for PV Systems under Partial Shading Condition. *Sensors*, 20(11), p. 3039. doi: 10.3390/s20113039.
- Sarwar, S., Hafeez, M. A., Javed, M. Y., Asghar, A. B. and Ejsmont, K. (2020). A Horse Herd Optimization Algorithm (HOA)-Based MPPT Technique under

- Partial and Complex Partial Shading Conditions. *Energies*, 15(5), p. 1880. doi: 10.3390/en15051880.
- Subudhi, B. and Pradhan, R. (2013). A Comparative Study on Maximum Power Point Tracking Techniques for Photovoltaic Power Systems. *IEEE Transactions on Sustainable Energy*, 4(1), pp. 89–98. doi: 10.1109/TSTE.2012.2202294.
- Sutikno, T., Samosir, A. S., Aprilianto, R. A., Purnama, H. S., Arsadiando, W. and Padmanaban, S. (2023). Advanced DC–DC Converter Topologies for Solar Energy Harvesting Applications: A Review. *Clean Energy*, 7, pp. 555–570. doi: 10.1093/ce/zkad003.
- Vangari, A., Haribabu, D. and Sakamuri, J. N. (2015). Modeling and control of DC/DC boost converter using K-factor control for MPPT of solar PV system. In: *2015 International Conference on Energy Economics and Environment (ICEEE)*, Greater Noida, India, September 2015. pp. 1–6.
- Villegas-Mier, C. G., Rodriguez-Resendiz, J., Álvarez-Alvarado, J. M., Rodriguez-Resendiz, H., Herrera-Navarro, A. M. and Rodríguez-Abreo, O. (2021). Artificial Neural Networks in MPPT Algorithms for Optimization of Photovoltaic Power Systems: A Review. *Micromachines*, 12(10), p. 1260. doi: 10.3390/mi12101260.
- Wang, Y., Li, Y. and Ruan, X. (2016). High-Accuracy and Fast-Speed MPPT Methods for PV String under Partially Shaded Conditions. *IEEE Transactions on Industrial Electronics*, 63(1), pp. 235–245. doi: 10.1109/TIE.2015.2465897.
- Yadav, D. and Singh, N. (2022). Intelligent techniques for maximum power point tracking. In: *Artificial Intelligence for Solar Photovoltaic Systems*, 105–127. doi: 10.1201/9781003222286-5.
- Yang, Y. and Wen, H. (2018). Adaptive Perturb and Observe Maximum Power Point Tracking with Current Predictive and Decoupled Power Control for Grid-Connected Photovoltaic Inverters. *Journal of Modern Power Systems and Clean Energy*, 7, pp. 422–432. doi: 10.1007/s40565-018-0437-x.
- Yung Yap, K., Sarimuthu, C. R. and Mun-Yee Lim, J. (2020). Artificial Intelligence Based MPPT Techniques for Solar Power System: A review. *Journal of Modern Power Systems and Clean Energy*, 8(6), pp. 1043–1059. doi: 10.35833/mpce.2020.000159.
- Zafar, M. H., Al-shahrani, T., Khan, N. M., Feroz Mirza, A., Mansoor, M., Qadir, M. U., Khan, M. I. and Naqvi, R. A. (2020). Group Teaching Optimization Algorithm Based MPPT Control of PV Systems under Partial Shading and Complex Partial Shading. *Electronics*, 9(11), p. 1962. doi: 10.3390/electronics9111962.